

# Effect of Changes of Variable Flavour Number Scheme on Parton Distribution Functions and Predicted Cross Sections

R.S. Thorne

Department Of Physics and Astronomy, University College London  
Gower Place, London, WC1E 6BT, UK  
E-mail: thorne@hep.ucl.ac.uk

## Abstract

I consider variations in the definitions, at next-to-leading order (NLO) and at next-to-next-to leading order (NNLO), of a General-Mass Variable Flavour Number Scheme (GM-VFNS) for heavy flavour structure functions. I also define a new “optimal” scheme choice improving the smoothness of the transition from one flavour number to the next. I investigate the variation of the structure function for a fixed set of parton distribution functions (PDFs) and also the change in the PDFs when a new MSTW2008-type global fit to data is performed for each GM-VFNS. At NLO the parton distributions, and predictions using them at hadron colliders, can vary by  $\sim 2 - 3\%$  from the mean value. At NNLO there is far more stability with varying GM-VFNS definition, and changes in PDFs and predictions are less than 1%, with most variation at very small  $x$  values. Hence, mass-scheme variation is an additional and significant source of uncertainty when considering parton distributions, but as with all perturbative uncertainties, it diminishes quickly as higher orders are included.

The treatment of heavy flavours in structure functions has a significant effect on the parton distribution functions (PDFs) obtained in fits to structure function, and other data, and consequently on the predictions for cross sections at hadron colliders such as the LHC and Tevatron. The up, down and strange quark are regarded as “light” quarks, and are always treated in the massless approximation since their current mass is much smaller than the regimes in which we use perturbative QCD. However, both the charm quark mass  $m_c$  and bottom quark mass  $m_b$  are much larger than  $\Lambda_{\text{QCD}}$  and so we can treat the generation of the charm and bottom parton distributions as a perturbative process. The details of the description of these heavy flavours, charm and bottom, in structure functions has an important impact on the PDFs extracted in fits, due both to the existence of direct data on  $F_2^h(x, Q^2)$ , where  $h$  represents the heavy quarks charm ( $c$ ) and bottom ( $b$ ), and also due to the contribution to the heavy quarks to the total structure function, particularly at small  $x$ . Indeed, using the published data [1] from the HERA experiment the latter of these is probably more important.

Traditionally there are two distinct regimes for heavy quark production using quite distinct theoretical descriptions. For  $Q^2 \sim m_h^2$  massive quarks are thought of as being created in the final state, and described using the Fixed Flavour Number Scheme (FFNS) (see [2] for NLO results),

$$F(x, Q^2) = C_k^{\text{FF}, n_f}(Q^2/m_h^2) \otimes f_k^{n_f}(Q^2), \quad (1)$$

where  $n_f$  is the number of light quark flavours. This does not sum  $\alpha_S^n \ln^n Q^2/m_h^2$  terms in the perturbative expansion, the consequence of which may well limit accuracy, though this is still a matter of debate. At high scales,  $Q^2 \gg m_h^2$ , heavy quarks behave like massless partons. The large logarithms mentioned can then be automatically summed via the solution of evolution equations for the heavy quark parton distributions. The distributions for different light quark number are related to each other via the perturbative expression

$$f_j^{n_f+1}(\mu_F^2) = A_{jk}(\mu_F^2/m_H^2) \otimes f_k^{n_f}(\mu_F^2), \quad (2)$$

where the matrix elements  $A_{jk}(\mu_F^2/m_H^2)$ , calculated at  $\mathcal{O}(\alpha_S^2)$  in [3] (and where calculations are ongoing at  $\mathcal{O}(\alpha_S^3)$  [4, 5, 6]), contain the fixed-order  $\ln(\mu_F^2/m_h^2)$  contributions. These expressions can be used at an appropriate choice of the factorisation scale, usually  $\mu_F^2 = m_h^2$  to obtain the boundary conditions for the evolution of the heavy flavour distribution, and simultaneously the change in the light parton distributions at this “transition point”. In the  $Q^2/m_h^2 \rightarrow \infty$  limit the description becomes the Zero-Mass Variable Flavour Number Scheme (ZM-VFNS),

$$F(x, Q^2) = C_j^{\text{ZMVF}, n_f+m} \otimes f_j^{n_f+m}(Q^2), \quad (3)$$

where  $m$  is the number of heavy quarks which have effectively become light quarks. Although called a “scheme” this is really an approximation until one reaches the real asymptotic limit since it ignores all  $\mathcal{O}(m_h^2/Q^2)$  corrections.

Various studies of comparisons between the FFNS and ZM-VFNS have been made. For the currently most obvious case of neutral current  $F_2^h(x, Q^2)$  it seems that the difference at NLO at high  $Q^2$  can be significant, but not enormous, see e.g. [7, 8, 9]. However, there are cases where the difference is more obvious, e.g.  $F_3^h(x, Q^2)$  in charged-current DIS [10, 11], and for example there is a distinct difference between the results using the two methods of calculation for the  $b$ -quark associated contribution to the  $Z$  cross-section in hadron-hadron colliders [12] and for the neutral supersymmetric Higgs boson [13], particularly for the largest boson masses. It seems natural to assume that the ZM-VFNS is more precise at very large scales, where resummation of large logarithms is most urgent, and that the FFNS is more precise for scales near  $m_h$ , where the ZM-VFNS is only an approximation. In order to correct this shortcoming in the ZM-VFNS but also sum the logarithms in  $Q^2/m_h^2$  (via explicit heavy quark parton distributions), and hence to obtain the most effective description between the two limits of  $Q^2 \leq m_H^2$  and  $Q^2 \gg m_H^2$ , one must use a General-Mass Variable Flavour Number Scheme (GM-VFNS).

A GM-VFNS is defined similarly to the ZM-VFNS, i.e. the structure function is written as

$$F(x, Q^2) = C_j^{\text{GMVF}, n_f+m}(Q^2/m_h^2) \otimes f_j^{n_f+m}(Q^2), \quad (4)$$

where now the coefficient functions are dependent on  $Q^2/m_h^2$ , but reduce to the zero mass limit as  $Q^2/m_h^2 \rightarrow \infty$ . If we consider the transition from  $n_f$  active quarks to  $n_f + 1$  then we can write

$$\begin{aligned} F(x, Q^2) &= C_j^{\text{GMVF}, n_f+1}(Q^2/m_h^2) \otimes f_j^{n_f+1}(Q^2) \\ &= C_j^{\text{GMVF}, n_f+1}(Q^2/m_h^2) \otimes A_{jk}(Q^2/m_h^2) \otimes f_k^{n_f}(Q^2) \equiv C_k^{\text{FF}, n_f}(Q^2/m_h^2) \otimes f_k^{n_f}(Q^2), \end{aligned} \quad (5)$$

and the GM-VFNS can be defined from the formal equivalence of the  $n_f$  flavour and  $n_f + 1$  flavour descriptions at all orders, resulting in

$$C_k^{\text{FF}, n_f}(Q^2/m_h^2) \equiv C_j^{\text{GMVF}, n_f+1}(Q^2/m_h^2) \otimes A_{jk}(Q^2/m_h^2), \quad (6)$$

where for simplicity I have set  $\mu_F^2 = Q^2$ . The fact that Eq.(2) correctly converts  $n_f$  flavour PDFs to  $n_f + 1$  flavour PDFs guarantees that at  $Q^2/m_h^2 \rightarrow \infty$ , where all power-suppressed  $m_h^2/Q^2$  corrections become negligible, the GM-VFNS coefficient functions become identical to the ZM-VFNS coefficient functions.

In order to illustrate the manner in which the GM-VFNS works we see that at  $\mathcal{O}(\alpha_S)$  Eq.(6) results in the equivalence

$$C_{2, hg}^{\text{FF}, n_f, (1)}(Q^2/m_h^2) = C_{2, h\bar{h}}^{\text{GMVF}, n_f+1, (0)}(Q^2/m_h^2) \otimes P_{qg}^0 \ln(Q^2/m_h^2) + C_{2, hg}^{\text{GMVF}, n_f+1, (1)}(Q^2/m_h^2), \quad (7)$$

(where  $(n)$  represents the  $n_{\text{th}}$  order in  $\alpha_S$  term of the coefficient function), which defines the GM-VFNS coefficient functions. As stated, the coefficient functions must tend to the massless limits as  $Q^2/m_h^2 \rightarrow \infty$ , and Eq.(7) is consistent with this. However,  $C_j^{\text{GMVF}}(Q^2/m_h^2)$  is only uniquely defined in this limit. One can swap  $\mathcal{O}(m_h^2/Q^2)$  terms between  $C_{2, h\bar{h}}^{\text{GMVF}, (0)}(Q^2/m_h^2)$  and  $C_{2, g}^{\text{GMVF}, (1)}(Q^2/m_h^2)$  in Eq. (7), and make similar swaps at higher order, i.e. as pointed out in [9] Eq. (6) is just an equivalence which can be used in the definition of a scheme, but has no unique solution since there are more free variables on the right-hand side of the equation than there are equations. (A similar observation was made independently in a slightly different context in [14], and presented very clearly and used to define a particularly efficient scheme in [15].) To show how the independence under changes of order  $\mathcal{O}(m_h^2/Q^2)$  works let us consider the expression for  $F_2^{h\bar{h}}$  up to  $\mathcal{O}(\alpha_S)$ .

$$\begin{aligned} F_2^{h\bar{h}} &= C_{2, h\bar{h}}^{\text{GMVF}, n_f+1, (0)}(Q^2/m_h^2) \otimes (h + \bar{h}) + \alpha_S C_{2, h\bar{h}}^{\text{GMVF}, n_f+1, (1)}(Q^2/m_h^2, \mu_F^2) \otimes (h + \bar{h}) \\ &+ \alpha_S \left( C_{2, hg}^{\text{FF}, n_f, (1)}(Q^2/m_h^2) - C_{2, h\bar{h}}^{\text{GMVF}, n_f+1, (0)}(Q^2/m_h^2) \otimes P_{qg}^0 \ln(\mu_F^2/m_h^2) \right) \otimes g, \end{aligned} \quad (8)$$

and let us assume that this is a particular well-defined GM-VFNS. Now we consider making a redefinition

$$C_{2, h\bar{h}}^{\text{GMVF}, n_f+1, (0)}(Q^2/m_h^2) \rightarrow C_{2, h\bar{h}}^{\text{GMVF}, n_f+1, (0)}(Q^2/m_h^2) + \delta C_{2, h\bar{h}}^{\text{GMVF}, n_f+1, (0)}(Q^2/m_h^2), \quad (9)$$

where  $\delta C_{2, h\bar{h}}^{\text{GMVF}, n_f+1, (0)}(Q^2/m_h^2)$  vanishes like a power of  $m - h^2/Q^2$  as  $Q^2/m_h^2 \rightarrow \infty$ . Under such a change in the coefficient function the change in the structure function is

$$\delta F_2^{h\bar{h}} = \delta C_{2, h\bar{h}}^{\text{GMVF}, n_f+1, (0)}(Q^2/m_h^2) \otimes (h + \bar{h}) - \alpha_S \delta C_{2, h\bar{h}}^{\text{GMVF}, n_f+1, (0)}(Q^2/m_h^2) \otimes P_{qg}^0 \ln(\mu_F^2/m_h^2) \otimes g. \quad (10)$$

From the relationship between the  $n_f + 1$  and  $n_f$  PDFs in Eq.(2) one can easily show that up to  $\mathcal{O}(\alpha_S)$ ,  $\delta F_2^{h\bar{h}} = 0$  (i.e.  $(h + \bar{h}) = \alpha_S P_{qg}^0 \ln(\mu_F^2/m_h^2) \otimes g + \mathcal{O}(\alpha_S^2)$ ). However, it is also useful to consider the renormalisation group equation in terms of factorisation scale  $\mu_F$ . Clearly a correctly defined structure function will have no dependence on  $\mu_F$ . Explicitly

$$\begin{aligned} \frac{d \delta F_2^{h\bar{h}}}{d \ln \mu_F^2} &= \delta C_{2,h\bar{h}}^{\text{GMVF},n_f+1,(0)}(Q^2/m_h^2) \otimes \frac{d(h + \bar{h})}{d \ln \mu_F^2} - \alpha_S \delta C_{2,h\bar{h}}^{\text{GMVF},n_f+1,(0)}(Q^2/m_h^2) \otimes P_{qg}^0 \otimes g + \mathcal{O}(\alpha_S^2), \\ &= \alpha_S \delta C_{2,h\bar{h}}^{\text{GMVF},n_f+1,(0)}(Q^2/m_h^2) \otimes (P_{qg}^0 \otimes g + P_{qq}^0 \otimes (h + \bar{h})) \\ &\quad - \alpha_S \delta C_{2,h\bar{h}}^{\text{GMVF},n_f+1,(0)}(Q^2/m_h^2) \otimes P_{qg}^0 \otimes g + \mathcal{O}(\alpha_S^2), \end{aligned} \quad (11)$$

and using the fact that  $(h + \bar{h})$  starts at  $\mathcal{O}(\alpha_S)$  we see that

$$\frac{d \delta F_2^{h\bar{h}}}{d \ln \mu_F^2} = 0 + \mathcal{O}(\alpha_S^2). \quad (12)$$

It can be shown explicitly that this feature exists to higher orders, but it is guaranteed from the definition Eq.(6) to work at all orders. At a finite order there is not exact cancellation, but the dependence on the choice of e.g.  $\delta C_{2,h\bar{h}}^{\text{GMVF},n_f+1,(m)}(Q^2/m_h^2)$ , will be higher order than that to which the structure functions are defined. For example, at NLO, where the  $\mathcal{O}(\alpha_S)$  coefficient functions are applied in the  $n_f + 1$  flavour regime, there is no cancellation in Eq.(10) between the NLO evolution of the charm distribution  $\propto \alpha_S^2 P_{qg}^1 \otimes g$  in the direct heavy flavour contribution and the coefficient function combined with gluon distribution contribution. However, this occurs when the  $\mathcal{O}(\alpha_S^2)$  coefficient functions are introduced at NNLO, and the uncanceled contribution is pushed to the evolution term  $\propto \alpha_S^3 P_{qg}^2 \otimes g$ . As we will see, this results in far more stable results under variation of GM-VFNS at NNLO than at NLO.

Perhaps the nomenclature ‘‘scheme’’ is misleading, since it suggests that one compensates for a change in coefficient functions with a change in PDFs, e.g. as when transforming from the  $\overline{\text{MS}}$  factorisation scheme to the DIS factorisation scheme. Here it is instead the case that because the heavy flavour is generated entirely from the gluon and light quarks via evolution (ignoring intrinsic flavour, which is discussed in [16]) there is an inherent ambiguity in exactly which contribution can be attributed to the heavy flavour and which to the light PDFs since one can be expressed precisely in terms of the other. It is only the fact that the large  $\ln(Q^2/m_h^2)$  terms are resummed in the heavy flavour distribution by evolution that stops the invariance under change of GM-VFNS being exact at finite order. Expressing  $(h + \bar{h})$  at the same order in  $\alpha_S$  as the coefficient functions, rather than as the full solution of the evolution equations would lead to exact invariance, but would be pointless as it would simply reproduce the results of the FFNS.

It should be noted that the freedom to modify coefficient functions by power suppressed terms, so long as this modification is applied to the corresponding subtraction terms, occurs separately in each structure function or cross-section. One may even change the GM-VFNS for  $F_2(x, Q^2)$  while leaving the one for  $F_L(x, Q^2)$  the same. The choice made in the fit to structure functions does not influence the choice made in predictions at hadron colliders, though at the moment most such predictions are at high enough scales that the zero-mass coefficients may

be used as a good approximation. This is certainly the case for data such as high- $E_T$  jets and  $W, Z$  production at the Tevatron and LHC currently used in global fits. The heavy flavour contribution to the cross section for fixed target Drell Yan data is extremely small so the total is insensitive to the heavy flavour prescription used. In principle some collider data would be best described using a GM-VFNS. There is no restriction on the form chosen from the manner in which the PDFs are fit (unless exactly the same data type is used in the fit, in which case there should be consistency). One would simply expect a *sensible* definition to be used for all data types. One clear criterion might be that all coefficient functions respect the correct kinematics to produce the physical final state containing the heavy quarks.

The freedom to define different definitions of a GM-VFNS has resulted in the existence of various prescriptions [8, 9, 17, 18, 19] each with a particular reasoning for the choice. The original ACOT scheme [8] simply calculated the heavy quark coefficient functions for single massive quark production and defined these to be  $C_{2,h\bar{h}}^{\text{GMVF},n_f+1}$ , hence defining the scheme. However, this required explicit calculation and also did not impose the correct kinematical requirement that (in neutral current DIS) one must have enough energy to create a pair of massive quarks in the final state. The TR GM-VFNS [9] highlighted the freedom in choice, and enforced correct kinematics via a definition which demanded the continuity of the value of  $dF_2^h/d\ln Q^2$  across the transition point. However, this was only possible in the gluon sector beyond  $\mathcal{O}(\alpha_S)$  and was quite complicated. The (S)ACOT( $\chi$ ) prescription [18] applied the simple choice

$$C_{2,h\bar{h}}^{\text{GMVF},(0)}(Q^2/m_h^2, z) \propto \delta(z - x_{\text{max}}), \quad (13)$$

which gives

$$F_2^{h,(0)}(x, Q^2) \propto e_h^2(h + \bar{h})(x/x_{\text{max}}, Q^2), \quad (14)$$

where  $x_{\text{max}} = Q^2/(Q^2 + 4m_h^2)$ , and imposes the threshold  $W^2 = Q^2(1-x)/x \geq 4m_h^2$ . This gives the usual limit

$$C_{2,h\bar{h}}^{\text{ZMVF},(0)}(z) = \delta(1-z) \quad (15)$$

for  $Q^2/m_h^2 \rightarrow \infty$ . The modified TR, or TR' scheme [19] adopted this and extensions to higher orders (though uses a different multiplicative factor of  $Q^2/(Q^2 + 4m_h^2)$  for the zeroth-order coefficient function [20]). Very recently the (S)ACOT( $\chi$ ) prescription has been extended explicitly to NNLO [21].

However, there is a further, more significant difference between the TR' scheme and the SACOT( $\chi$ ) scheme. ACOT-type schemes have used the same order of  $\alpha_S$  above and below the transition point  $Q^2 = m_h^2$ , despite the fact that FFNS is LO at  $\mathcal{O}(\alpha_S)$  while the ZM-VFNS starts at zeroth order. Instead the TR' definition uses, for example, at LO the  $\mathcal{O}(\alpha_S)$  FFNS result for  $Q^2 < m_h^2$ , and for  $Q^2 > m_h^2$

$$F_2^h(x, Q^2) = \alpha_S(m_h^2)C_{2,hg}^{\text{FF},n_f,(1)}(Q^2 = m_h^2) \otimes g^{n_f}(Q^2 = m_h^2) + C_{2,h\bar{h}}^{\text{GMVF},n_f+1,(0)}(Q^2/m_h^2) \otimes (h + \bar{h})(Q^2), \quad (16)$$

i.e. it freezes the higher order  $\alpha_S$  term when going upwards through  $Q^2 = m_h^2$ . This difference in choice can be phenomenologically important in the vicinity of  $Q^2 = m_h^2$ , though becomes less important at high  $Q^2$  as the frozen term becomes smaller compared to the growing contribution

from the heavy quark distribution. The effect is quite significant at small  $x$  at NLO, since the  $\mathcal{O}(\alpha_S^2)$  contribution  $\alpha_S^2 C_{2,cg}^{\text{FF},\text{nf},(2)} \otimes g^{nf}$  is large for  $Q^2 \sim m_h^2$ , as seen in Fig. 2 of [19].

There is also an alternative, but ultimately equivalent, way of formulating a GM-VFNS, where instead of having a transition point where one turns on heavy quark distributions and defining GM-VFNS coefficient functions one obtains the total structure function from a variety of contributions which cancel each other appropriately to obtain the correct limits in the low and high  $Q^2$  regimes. The BMSN (Buza, Matiounine, Smith and van Neerven) [3] and FONLL (fixed-order next-to-leading log) [20] definitions for a scheme are based on the expression

$$F^{\text{GMVF}}(x, Q^2) = F_2^{\text{FF}}(x, Q^2) - F_2^{\text{asympt}}(x, Q^2) + F_2^{\text{ZMVf}}(x, Q^2), \quad (17)$$

where generally speaking the second (subtraction) term is the asymptotic version of the first, i.e. all terms of  $\mathcal{O}(m_h^2/Q^2)$  are omitted. There are differences in exactly how the second and third terms are defined in detail in different schemes. In the standard applications the  $\alpha_S$  order of  $F_2^{\text{FF}}(x, Q^2)$  at low  $Q^2$  is the same as that of  $F_2^{\text{ZMVf}}(x, Q^2)$  as  $Q^2 \rightarrow \infty$ . This type of scheme is used in [23] using  $\mathcal{O}(\alpha_S)$  coefficient function expressions along with LO PDFs, and  $\mathcal{O}(\alpha_S^2)$  coefficient function expressions along with NLO PDFs. However, ultimately the FFNS scheme is used for structure functions in fitting to structure function data,  $\mathcal{O}(\alpha_S^2)$  for both NLO and NNLO fits (approximate  $\mathcal{O}(\alpha_S^3)$  coefficient functions, and a running quark mass, are used in [24] and [25]). The FONLL approach, which modifies  $F_2^{\text{asympt}}(x, Q^2)$  and  $F_2^{\text{ZMVf}}(x, Q^2)$  by, for example, the replacement of  $x$  by  $\chi$  in order to maintain correct kinematics in each term, is used at NLO in [26] and at LO and NNLO in [27]. By default the order of  $\alpha_S$  is the same in each of the three terms and the GM-VFNS uses  $\mathcal{O}(\alpha_S^0)$  coefficient function expressions along with LO PDFs,  $\mathcal{O}(\alpha_S)$  coefficient function expressions along with NLO PDFs and  $\mathcal{O}(\alpha_S^2)$  coefficient function expressions along with NNLO PDFs. There is a version of FONLL, FONLL-B, which uses one power higher in the FFNS and subtraction term, but where the subtraction term contains only the  $\ln(Q^2/m_h^2)$  terms, not the finite part, so that at  $Q^2 = m_h^2$ ,  $F^{\text{GMVF}}(x, Q^2) \equiv F_2^{\text{FF}}(x, Q^2)$ . This reproduces the correct NLO FFNS at  $Q^2$  near to threshold, but unlike the case where the coefficient functions are  $\mathcal{O}(\alpha_S)$  in all pieces it leads to part (but not all) of the higher order NNLO contribution persisting as  $Q^2 \rightarrow \infty$ , i.e.  $F_2^{\text{FF}}(x, Q^2)$  and  $F_2^{\text{asympt}}(x, Q^2)$  do not cancel in this limit so the exact  $F_2^{\text{ZMVf}}(x, Q^2)$  is accompanied by a formally subleading term, reminiscent (but different in origin and form) of the frozen contribution in the TR' approach.

Ideally one would like any GM-VFNS to reduce to exactly the correct order FFNS at low  $Q^2$  and exactly the correct order (one power of  $\alpha_S$  lower) ZM-VFNS as  $Q^2 \rightarrow \infty$ . At present, as outlined above, none do. However, in the case of the TR' scheme this can easily be rectified. The fact that the higher- $\alpha_S$  order term is frozen for  $Q^2 > m_h^2$  was strictly necessary in the original TR scheme in order to impose exact continuity of  $dF_2^h/d\ln Q^2$ . However, this is no longer a requirement, so rather than this term being frozen it could instead be of the form

$$(m_h^2/Q^2)^a \alpha_S^n(m_h^2) \sum C_{2,i}^{\text{FF}}(m_h^2) \otimes f_i(m_h^2) \quad \text{or} \quad (m_h^2/Q^2)^a \alpha_S^n(Q^2) \sum C_{2,i}^{\text{FF}}(Q^2) \otimes f_i(Q^2). \quad (18)$$

Any  $a > 0$  provides the correct asymptotic limit, though strictly from factorization one should have  $(m_H^2/Q^2)$  times  $\ln(Q^2/m_H^2)$  terms. Fractional values of  $a$  could be thought of as mimicking the power times logarithmic corrections. As well as modifying the previously frozen term in this

scheme	a	b	c	d
GM-VFNS1	0	-1	1	0
GM-VFNS2	0	-1	0.5	0
GM-VFNS3	1	0	0	0
GM-VFNS4	0	0.3	1	0
GM-VFNS5	0	0	0	0.1
GM-VFNS6	0	0	0	-0.2
optimal	1	-2/3	1	0

Table 1: The values of parameters defined in Eqs.(18,19,20) for different extreme GM-VFNS definitions.

manner there is also more freedom in the definition of the GM-VFNS than previously used or explored. Indeed, this freedom is an inherent feature of a GM-VFNS, so its consequences should be investigated quantitatively.

One can modify the heavy quark coefficient function so long as the correct  $Q^2/m_h^2 \rightarrow \infty$  limit is maintained. However, since this appears in convolutions for higher order subtraction terms, it is desirable to avoid a complicated  $x$  dependence. A simple choice is

$$C_{2,h\bar{h}}^{\text{GMVF},(0)}(Q^2/m_h^2, z) \rightarrow (1 + b(m_h^2/Q^2)^c)\delta(z - x_{\text{max}}), \quad (19)$$

where again variation in  $c$  really mimics  $(m_h^2/Q^2)$  with logarithmic corrections. One can also modify the argument of the  $\delta$ -function, similar to the Intermediate-Mass IM scheme [22], we can define

$$\xi = x/x_{\text{max}} \rightarrow x(1 + (x(1 + 4m_h^2/Q^2))^d 4m_h^2/Q^2), \quad (20)$$

so the kinematic limit stays the same, but if  $d > 0$  ( $< 0$ ) small  $x$  is less (more) suppressed. The default  $a, b, c, d$  are all zero, but can vary, being limited by fit quality or *sensible* choices, e.g. we would not choose  $b < -1$ , since this would give a negative zeroth-order heavy quark coefficient function near  $Q^2 = m_h^2$ . There is also a potential source of uncertainty from variation of the transition scale away from  $\mu^2 = m_h^2$ . However, much of the type of possible variation in  $F_2^h$  is very similar to that obtained by the variation of parameters already described.

A variety of different choices defined in Table 1 has been tried at NLO and at NNLO, along with the ZM-VFNS (at NLO).<sup>1</sup> The resulting variations in  $F_2^c(x, Q^2)$  near the transition point due to different choices of GM-VFNS at NLO are shown in the left of Fig. 1. (A similar variation under changes in scales and scaling variable has appeared in [21].) I also define an “optimal” scheme which is chosen to be smooth at threshold, at NLO, and reduces to exactly the right limits at high and low  $Q^2$ . There is quite a spread in the values of  $F_2^h(x, Q^2)$  at NLO, though the ZM-VFNS is far steeper at low  $Q^2$  than any GM-VFNS. The continuation of the FFNS result above  $Q^2 = m_h^2$  is also shown at NLO, and it is clear that at both  $x$  values all GM-VFNS variations are ultimately rising above this. In the vicinity of  $Q^2 = m_h^2$  the optimal scheme stays closest to FFNS. The spread is very much reduced at NNLO, the right of Fig. 1, with almost

<sup>1</sup>Some of the results from this were presented in [28].

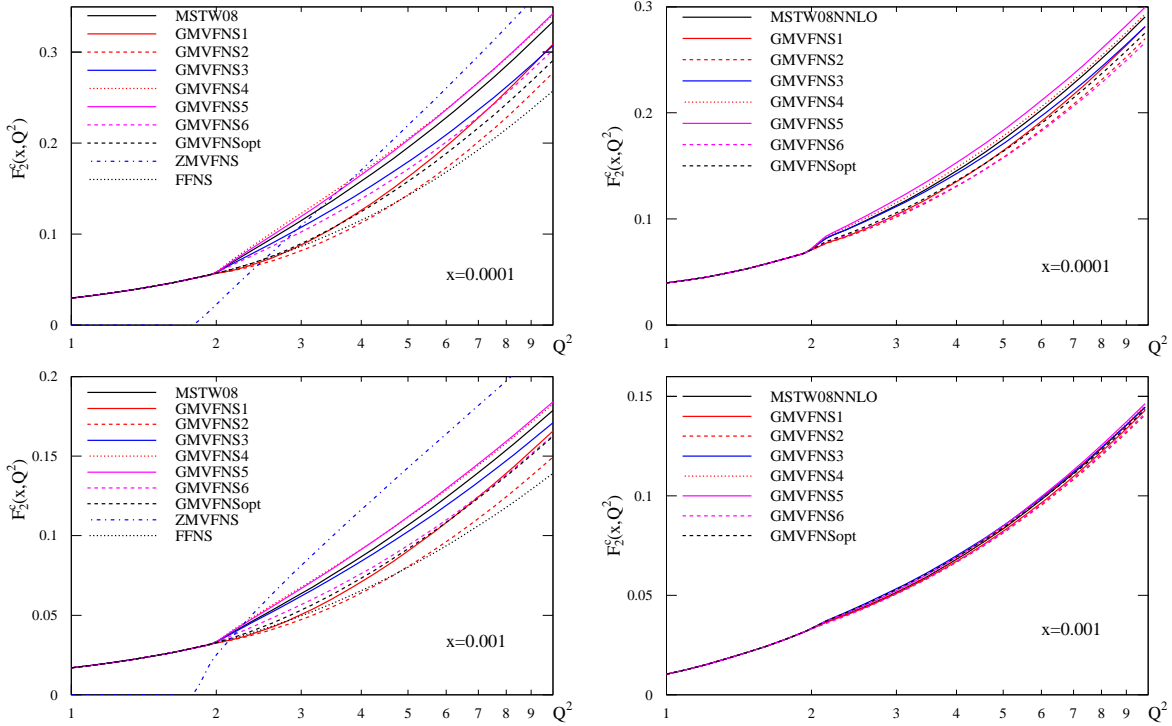


Figure 1: The variation in  $F_2^c(x, Q^2)$  generated from a variety of choices of GM-VFNS at NLO (left) and NNLO (right) using the MSTW2008 pdfs in each case.

zero variation until very small  $x$ . At this point the precise cancellation between different terms in the expression for the GM-VFNS near the transition point is starting to fail to some extent, showing that NNLO evolution effects are most important in this regime and even higher orders in the GM-VFNS are needed for there to be very little sensitivity to choices. The FFNS is not shown in this case as the NNLO ( $\mathcal{O}(\alpha_s^3)$ ) contribution to this is only approximate and it is possible, and arguably likely, that the approximation is worse away from the  $Q^2 \sim m_h^2$  regime where it is important in the GM-VFNS.

Global fits are also performed using the same procedure as the MSTW2008 fit [29] for all schemes, and the value of  $\alpha_s(M_Z^2)$  is allowed to vary in all cases. At NLO the initial  $\chi^2$  for a new GM-VFNS can change by up to 250, but converges to within 20 of the original with refitting. The fit is improved for options 1, 2 and 6, and the optimal scheme and the fit is best for the option 6, where it is 23 units lower than for the best fit in [29] – in particular the quality of fit to the HERA  $F_2^c$  data improves from 110 to 90 for 83 points. For option 2, the fit quality is almost unchanged. For options 4 and 5 the values of  $b$  and  $d$  respectively are limited by the quality of fit of the HERA  $F_2^c$  data, i.e. we stop variations when the fit quality reaches 7 units higher than the best fit for MSTW2008. The variations in the partons extracted at NLO are shown in the left of Fig. 2. The default TR' scheme sits near the low end at small  $x$  values. Some changes in PDFs exceed the one  $\sigma$  experimental PDF uncertainty in the upwards direction at small  $x$ .  $\alpha_s(M_Z^2)$  changes by  $< 0.0007$  for all variations of the GM-VFNS, only about half the



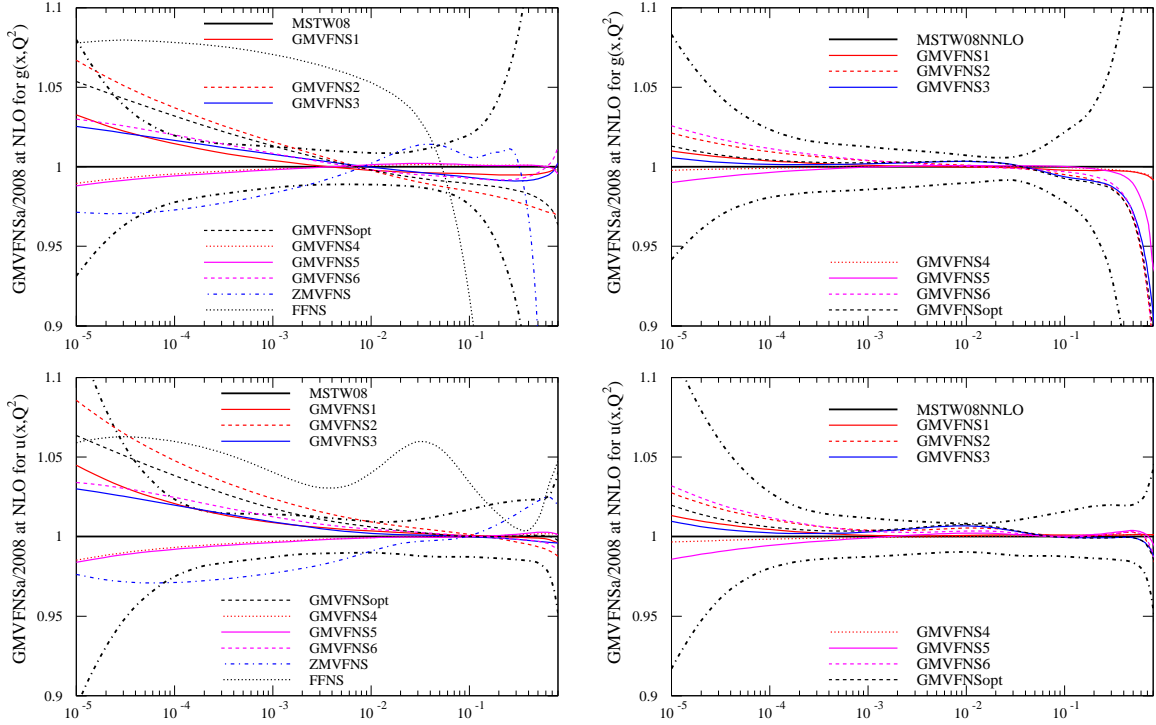


Figure 2: The variation of the gluon (upper plots) and quark (lower plots) PDFs at  $Q^2 = 10,000\text{GeV}^2$  obtained from the best fit from a variety of choices of GM-VFNS, the ZM-VFNS and the FFNS at NLO (left) and the GM-VFNS variations at NNLO (right) as a ratio to the MSTW2008 PDFs. The one-sigma uncertainties for the MSTW2008 PDFs are shown as dash-dotted lines.

PDF set	Tevatron		LHC (7 TeV)		LHC (14 TeV)	
	$\sigma_Z$ (nb)	$\sigma_H$ (pb)	$\sigma_Z$ (nb)	$\sigma_H$ (pb)	$\sigma_Z$ (nb)	$\sigma_H$ (pb)
MSTW2008	7.207	0.7462	27.70	12.41	59.25	40.69
GMvar1	+0.3%	-0.5%	+0.7%	-0.1%	+1.1%	+0.2%
GMvar2	+0.7%	-1.1%	+2.0%	+0.5%	+3.0%	+1.5%
GMvar3	+0.1%	-0.3%	+0.7%	+0.4%	+1.1%	+0.8%
GMvar4	+0.0%	-0.1%	-0.3%	-0.1%	-0.4%	-0.2%
GMvar5	-0.1%	-0.1%	-0.4%	-0.2%	-0.5%	-0.3%
GMvar6	+0.3%	-0.4%	+1.0%	+0.3%	+1.6%	+0.8%
GMvaropt	+0.3%	-1.5%	+1.5%	+0.1%	+2.0%	+0.4%
ZM-VFNS	-0.7%	-1.2%	-1.6%	-1.8%	-3.0%	-3.1%
FFNS - DIS only	+3.1%	-14.4%	+4.5%	-0.7%	+7.0%	+3.0%
GMvarcc	+0.0%	-0.1%	+0.0%	-0.1%	+0.0%	-0.1%

Table 2: Predicted cross-sections at NLO for  $Z$  and a 120 GeV Higgs boson at the Tevatron and LHC.

experimental uncertainty found in [30].<sup>2</sup> I also perform a fit using the ZM-VFNS. In this case the value of  $\alpha_S(M_Z^2)$  falls by 0.0015. The ZM-VFNS PDF is clearly outside the GM-VFNS band in some places. The fit quality is about 200 units worse than the MSTW2008 fit. 130 of this is the fit to the  $F_2^c(x, Q^2)$  data which is very poorly fit at low  $Q^2$  and much of the rest is from a worse fit to HERA structure function data. There is little difference in the fit if the charm structure function data are omitted.

It is also interesting to investigate a fit in the FFNS scheme. In this case it is not possible to perform a full global fit since the coefficient functions are not fully known for hadron-hadron collider processes even at NLO. It would be possible to perform a hybrid fit where for structure functions we stayed with the three flavour description but for collider data let the same partons evolve in a variable flavour scheme. However, this seems a peculiar compromise - either one attempts to resum the logarithms or one does not. Hence, I consider a FFNS fit to structure function data only, also omitting the high- $Q^2$  charged current HERA data, which also rely on not fully known coefficient functions at order  $\alpha_S^2$ . The resulting fit has  $\chi^2 = 1944/2089$ , compared to  $\chi^2 = 1878/2089$  for the MSTW2008 fit, i.e. the contribution of the the  $\chi^2$  from these data to the full MSTW2008 fit, not a new fit to the restricted data set. A new fit using the default GM-VFNS gives an improvement of about 30 units and only minor changes in PDFs. The improvement is mainly due to some reshuffling of the flavours with no Drell Yan data constraint allowing a better fit to the fixed target DIS data. There is little change for HERA data. The fit using the FFNS has a value of  $\alpha_S(M_Z^2)$  of 0.1187 when it is evolved from low scales in a variable flavour scheme, 0.0025 lower than the MSTW value. This lower value allows a better fit to BCDMS data, but there is a deterioration in the fit to NMC data, to the nuclear target neutrino DIS data and the the HERA data at higher  $Q^2$  where  $F_2(x, Q^2)$  does not rise as quickly with  $Q^2$  as in the GM-VFNS. The fit to  $F_2^c(x, Q^2)$ , for which the most precise data is at relatively low  $Q^2$ , is slightly better in the FFNS, but this is far from compensating for the deteriorations elsewhere. The partons obtained in the FFNS fit are qualitatively different to those in the GM-VFNS fit. The gluon distribution is larger at small- $x$  and correspondingly lower at high- $x$ . This is qualitatively very similar to the difference between the gluon distribution in the ABKM PDF set [23] (or more recently [25]), which uses the FFNS and the MSTW set, as is the change in the coupling constant. At small- $x$  this difference in the gluon shape is reflected in the quarks at higher  $Q^2$  since their evolution is determined mainly by the gluon. The input PDFs in the FFNS fit can be evolved using a variable flavour scheme in order to make a more direct comparison at high- $Q^2$  possible, and to examine the compatibility with collider data. The ratio to the MSTW2008 PDFs can be seen in the left of Fig. 2, and it is clear they are qualitatively different. The predictions for Tevatron jet data are very poor, and there is a distinct deterioration in the fit quality for the  $Z$  rapidity data from CDF. In contrast the DIS-only fit using the GM-VFNS gives predictions for Tevatron jet data that have  $\chi^2$  values only a few units higher than when these data are included, and the prediction for the  $Z$  rapidity data is actually marginally better than the global fit. Clearly at NLO the results from the FFNS and any GM-VFNS are rather

---

<sup>2</sup>A comparison between GM-VFNS definitions of different groups using a common set of PDFs can be found in [31], and more complete comparisons are in progress. The differences are well-understood. At low  $Q^2$  some of the differences are bigger than those exhibited in this article, but this is due to the different ordering chosen by different groups in the  $Q^2 < m_h^2$  region which is a fixed part of our definition.

different. One would expect this difference to diminish at higher orders, but a precise comparison awaits the full calculation of FFNS coefficient functions.

The variation in GM-VFNS is also applied to the charged-current cross-section expressions. None of the variations in  $a, b, c, d$  of the form already considered lead to changes in the  $\chi^2$  of much greater than one unit even before refitting. The change in the PDFs with refitting is largest for the strange quark, which is probed by dimuon production which relies on the heavy flavor formalism, but is always very much smaller than 1%. This is due to the fact that the changes in structure function with change in scheme definition are by far most significant at small  $x$ , and the charged current data is all for  $x > 0.01$ . It is also because in the charged-current case one only produces a single heavy particle in the final state, i.e. the threshold  $W^2 = m_h^2$  rather than  $4m_h^2$  so there is less sensitivity to how the massless limit is approached than the neutral current case. Finally, the data on dimuon production is a combination of the structure functions  $F_2(x, Q^2)$ ,  $F_L(x, Q^2)$  and  $F_3(x, Q^2)$ , each with a particular  $y$  dependence. In practice the contribution from the charm quark contribution and the corresponding gluon subtraction term are suppressed by a factor of  $(1 - y)^2$ . For these data  $0.3 < y < 0.7$  so this factor is always significantly less than 1, and moreover the contribution with larger charm quark or subtraction are at larger  $y$  and most suppressed.<sup>3</sup>

The predictions for cross-sections are shown at NLO in Table. 2. It is assumed that any  $\mathcal{O}(m_{c,b}^2/m_{Z,H}^2)$  corrections which would occur in a full GM-VFNS definition are negligible and the ZM-VFNS result is used. There is at most a 1.5% variation at the Tevatron. At the recent energy at the LHC of 7 TeV there is a variation of +2% to -0.4% in  $\sigma_Z$ . This is increased to +3% to -0.5% at 14 TeV due to smaller  $x$  being sampled. The spread in  $\sigma_H$  at the LHC is about halved compared to  $\sigma_Z$  due to the higher average  $x$  sampled. The ZM-VFNS is a clear outlier in the low direction at the LHC. However, the ZM-VFNS variations are only about 3% at most compared to our default, and never more than 5% even compared to the most upward GM-VFNS variations. Hence, the ZM-VFNS change is more similar to that observed by NNPDF when adopting a GM-VFNS to obtain PDFs [26], than the larger changes observed by CTEQ when adopting a GM-VFNS as default for the first time [32]. The FFNS predictions are also shown, and display some rather large variations, particularly in the Tevatron Higgs cross section. However, it should be remembered that this is a fit to a more limited data set than all the others. It is, however, indicative of the major differences seen between MSTW2008 PDFs and some PDFs obtained using fits using the FFNS. GMvarcc denotes variation in the GM-VFNS for charged current processes, and clearly the effect is very small indeed.

For fits at NNLO the initial changes in  $\chi^2$  are much smaller than at NLO, i.e.  $< 20$ , and they converge to within 10 of the original. In fact they are all within 2-3 units of the default fit except for options 2 and 6 where the fit quality is about 10 worse. In fact for option 6 the variation of the  $d$  parameter is limited by the deterioration in the fit to the HERA  $F_2^c$  data in the NNLO fit rather than NLO. The variations in the PDFs extracted at NNLO are shown in the right of Fig. 2. At the very worst the changes approach the one  $\sigma$  experimental PDF

---

<sup>3</sup>There is the related issue of how diagrams where the final state charm quark is generated away from the parton-boson interaction vertex should be considered in dimuon production, which is done differently by different groups and related to the acceptance corrections. This should be clarified, but is a separate topic to the particular scheme variations considered in this article. The suppression noted above makes the effect very small, however.

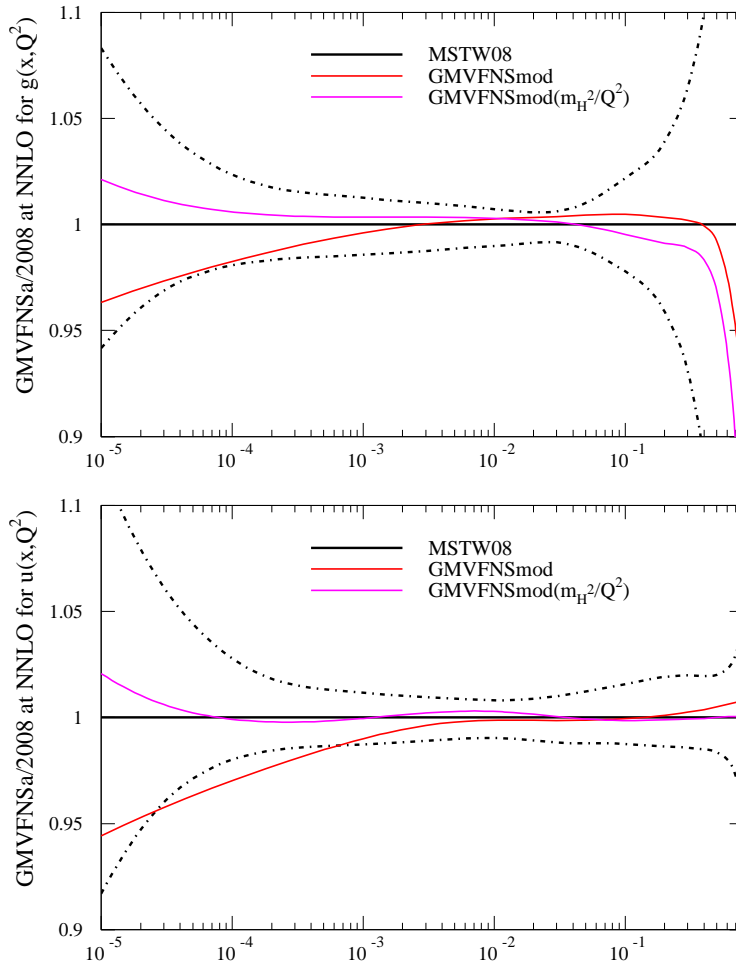


Figure 3: The variation in PDFs at  $Q^2 = 10,000\text{GeV}^2$  obtained from two choices of GM-VFNS at NNLO where the coefficient of the unknown constant in the small- $x$  term in the  $\mathcal{O}(\alpha_S^3)$  part of the FFNS coefficient function is taken to its extreme value. In one case it is frozen for  $Q^2 > m_c^2$  and in the other it falls like  $m_c^2/Q^2$ .

uncertainty, but are usually far less. Variations in  $\alpha_S(M_Z^2)$  are  $\sim 0.0003$ . Hence, the stability of the PDFs to variations in the parameters  $a, b, c, d$  defining how quickly the heavy flavour PDF turns on, and correspondingly the size of subtraction terms, diminishes greatly at NNLO due to increased cancellation of the two types of term.

However, at NNLO there is another source of uncertainty associated with the GM-VFNS definition. The TR' scheme models the  $\mathcal{O}(\alpha_S^3)$  FFNS terms at low  $Q^2$  using known leading threshold logarithms [33] and  $\ln(1/x)$  terms [34]. The small- $x$  model takes the form

$$A(Q^2/m_h^2)(1 - z/x_{\text{max}})^{\tilde{a}}(\ln(1/z) - \tilde{b})/z, \quad (21)$$

where  $A(Q^2/m_h^2)$  is a calculated function, but  $\tilde{a}$  and  $\tilde{b}$  are free parameters determining at what  $x$  the leading  $\ln(1/x)$  contribution becomes dominant. The default values are  $\tilde{a} = 20, \tilde{b} = 4$ , but  $\tilde{a}$

PDF set	Tevatron		LHC (7 TeV)		LHC (14 TeV)	
	$\sigma_Z$ (nb)	$\sigma_H$ (pb)	$\sigma_Z$ (nb)	$\sigma_H$ (pb)	$\sigma_Z$ (nb)	$\sigma_H$ (pb)
MSTW2008	7.448	0.9550	28.53	15.71	60.93	50.51
GMvar1	+0.1%	-0.5%	+0.1%	-0.3%	+0.1%	-0.2%
GMvar2	+0.3%	-0.8%	+0.2%	+0.1%	+0.5%	+0.1%
GMvar3	+0.4%	-0.1%	+0.4%	+0.6%	+0.5%	+0.7%
GMvar4	+0.0%	-0.2%	-0.1%	-0.1%	+0.1%	-0.1%
GMvar5	+0.1%	-0.3%	-0.1%	-0.2%	-0.2%	-0.2%
GMvar6	+0.1%	-0.9%	+0.0%	-0.5%	+0.3%	-0.2%
GMvaropt	+0.4%	-0.2%	+0.5%	+0.6%	+0.6%	+0.8%
GMvarmod	-0.2%	-0.4%	-0.8%	-0.6%	-1.4%	-1.0%
GMvarmod'	+0.0%	-0.7%	+0.0%	+0.0%	+0.0%	+0.1%

Table 3: Predicted cross-sections at NNLO for  $Z$  and a 120 GeV Higgs boson at the Tevatron and LHC.

and  $\tilde{b}$  can be varied. Changes in  $\tilde{a}$  within reasonable limits make little difference. The maximum *sensible* variation of  $\tilde{b} = 2$  (determined by the fact that the fit quality is not significantly altered, similar to the variations of  $a$ - $d$ ) leads to an effect of order the experimental PDF uncertainty at  $x \leq 0.001$ , as shown in Fig. 3. However, this change in the PDFs is largely eliminated if the  $\mathcal{O}(\alpha_S^3)$  contribution dies away like  $m_h^2/Q^2$ , rather than being frozen, as also seen in Fig. 3. This is another reason for preferring this choice.

The changes in predictions for cross sections at NNLO are seen in Table. 3. Other than model dependence – GMvarmod denotes the variation to  $\tilde{b} = 2$  in the  $\mathcal{O}(\alpha_S^3)$  term – which reaches slightly more than 1% for 14 TeV at the LHC, the maximum variations are of order 0.5% at LHC. GMvarmod' is when the  $\mathcal{O}(\alpha_S^3)$  terms fall with  $Q^2$ , and clearly exhibits a very small deviation. Hence, as the changes in PDFs essentially guaranteed, there is far less uncertainty in predictions for cross sections due to uncertainties in definitions of the GM-VFNS at NNLO than at NLO, exactly as we would expect for a theoretical ambiguity due only to the finite order at which one is working. The reduction in uncertainty is exactly as (usually) observed for scale variations.

As a point of detail I note that at even at NNLO the smoothness across the transition point exhibited in the right of Fig. 1 is not ideal. This is not so surprising at  $x = 10^{-4}$  since as noted a new  $\ln(1/x)$  divergence in the evolution of the heavy quark is introduced into the quark evolution at NNLO which is not effectively cancelled by the subtraction terms. However, at  $x = 0.001$  the slope immediately above the transition point is slightly flatter than below it. This is the same for all variations of the GM-VFNS, so in fact is not a feature of the definition of a GM-VFNS at all. It can be traced to the behaviour below  $Q^2 = m_h^2$ , i.e. to the modelling of the  $\mathcal{O}(\alpha_S^3)$  coefficient function. In the small- $x$  part of this in Eq. (21) it is assumed that the  $Q^2/m_h^2$  dependence of the constant term  $\tilde{b}$  is the same as the known  $\ln(1/x)$  term. Modifying this by a rather slowly varying factor of  $(Q^2/m_h^2)^{0.1}$  results in the rather smoother behaviour shown in Fig. 4. Hence, this might be thought of as an improvement to this  $\mathcal{O}(\alpha_S^3)$  coefficient function.

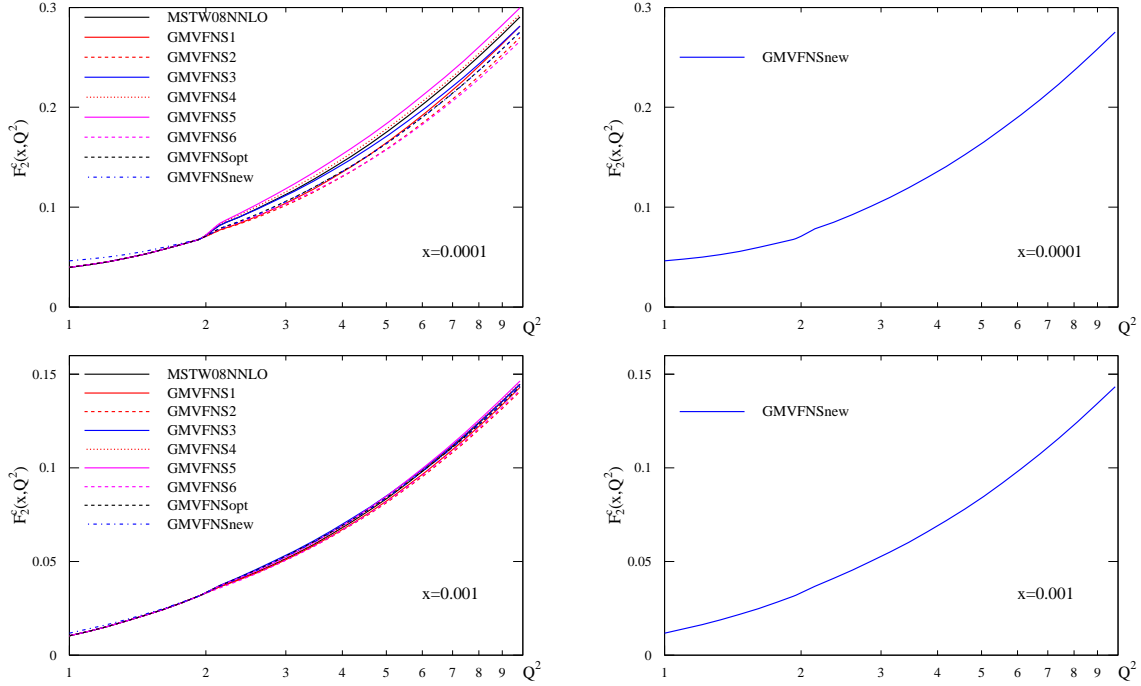


Figure 4: The variation in  $F_2^c(x, Q^2)$  generated from a variety of choices of GM-VFNS at NNLO where the low  $Q^2$  modelling has been modified in one, improving the smoothness at the transition point (left-hand plots). In the right-hand plots only this choice is shown for clarity.

However, it affects the structure functions only below  $Q^2 = m_c^2$  for the charm contribution, i.e. below the MSTW2008  $Q^2$  cut, and the influence from the change in the very small amount of  $F_2^b$  for  $Q^2 < m_b^2$  is very minor. Even without refitting the global fit changes by only about 1 unit, and so no significant change in PDFs occurs. More important, but very similar in practice, is an improvement in threshold corrections which could be made in the same term. Since the publication of the MSTW2008 PDFs more logarithms in the threshold correction have been calculated, see [35]. These can be included in the  $\mathcal{O}(\alpha_s^3)$  coefficient function (though some approximation is needed since in [35] the value of one coefficient is presented only for specific  $m_c^2/Q^2$  values, though the full result very recently appeared in [36]). The result is that this improvement itself makes the behaviour at the transition point smoother, and leads to a small modification of the structure function both below, and at the transition point. The change at the transition point then persists as a constant if this term is frozen, though becomes relatively less important very rapidly, or quickly disappears if this term is defined to fall away like  $m_h^2/Q^2$ . Hence, even though this improvement will be included in future schemes, and is beneficial to the detailed behaviour of the structure function, within this definition of an NNLO GM-VFNS the effect on the PDFs is extremely small.

Finally, it is an interesting question whether the changes in the GM-VFNS have any influence on the value of the quark masses preferred by the MSTW2008 fits, as presented in [12]. As noted in this previous study there is little constraint on  $m_b$  from fits, and indeed there is very little sensitivity to the GM-VFNS definition. However, there is a distinct effect on the conclusions

regarding  $m_c$  (see also [37]). The default MSTW2008 choice of charm mass  $m_c = 1.4\text{GeV}$  is chosen to be near the best fit value at NLO, which turns out to be  $m_c = 1.45\text{GeV}$  with a very marginally better fit quality than  $m_c = 1.4\text{GeV}$ . The same default mass is used in the studies in this article to enable direct comparison to MSTW2008 results. However, when  $m_c$  is allowed to vary using the optimal scheme at NLO the best fit value is for  $m_c = 1.32\text{GeV}$ , and the quality of the fit is 11 units better than for  $m_c = 1.4\text{GeV}$  and 17 units better than the best fit for  $m_c = 1.45\text{GeV}$  using the default scheme. The fit does prefer the smoother behaviour near the transition point in the optimal scheme, but the slower turn on of  $F_2^c$  at low  $Q^2$  results in a preference for a lower mass. The variation with scheme is much less at NNLO, and correspondingly the variation in the best fit mass is also smaller. It changes from  $m_c = 1.26\text{GeV}$  in [12] to  $m_c = 1.23\text{GeV}$  using the optimal scheme. The best fit quality for the preferred mass is 7 units lower using the optimal scheme at NNLO. Hence, the difference in the values for the pole charm mass extracted at NLO and NNLO has reduced from  $0.19\text{GeV}$  in [12], to  $0.09\text{GeV}$  using the optimum scheme, and both NLO and NNLO fits are within their uncertainty for  $m_c$  for an intermediate value of  $m_c = 1.28\text{GeV}$ . Compatibility is certainly improved, but the values are rather low, a trend also seen for the charm mass defined in  $\overline{\text{MS}}$  scheme extracted from fits to structure function data in [24]. There is some evidence in this study that the convergence of the perturbation series in the FFNS is quicker when using the  $\overline{\text{MS}}$  scheme definition of the mass than when using the pole mass as is used in this study and is currently the most common framework. It would certainly be interesting to investigate this in the context of GM-VFNS analyses. However, the situation is not quite the same in a GM-VFNS. The first dependence on scheme occurs for coefficient functions at order  $\alpha_S^2$ . Hence, for many GM-VFNS definitions, e.g. any ACOT variation and the default NNPDF choice, the mass-scheme dependence would not set in until NNLO. For our definition the  $\alpha_S$  coefficient functions only play a minor role at low  $Q^2$ , being either frozen at  $Q^2 = m_h^2$  or falling away quickly in the new optimal scheme. Hence, the mass-scheme dependence will be less influential at NLO in the GM-VFNS than in the FFNS, particularly in the optimal scheme. At NNLO the  $\alpha_S^2$  coefficient functions are used at all scales, so the mass-scheme dependence will come into play fully. However, at low  $Q^2$  where the mass-scheme dependence is undoubtedly most important there is the additional uncertainty due to the lack of the full  $\mathcal{O}(\alpha_S^3)$  coefficient functions, so it is uncertain how much information the mass-scheme dependence can currently provide.

To summarise, I have considered variations in the definition of a GM-VFNS within the framework used in MSTW, and various other global fits for PDFs. In particular I have noted that none (in any framework) currently reduce to *exactly* the appropriate order FFNS expression at low  $Q^2$  and also the appropriate order ZM-VFNS expression as  $Q^2/m_h^2 \rightarrow \infty$ , though I have shown this can be easily achieved in the TR' scheme. I have investigated the variation of both the heavy flavour structure function obtained and the PDFs extracted when 4 parameters controlling the definition of the GM-VFNS are varied within limits set by fit quality or sensible behaviour at NLO and NNLO. At NLO, variations in the resulting PDFs can be similar to the experimental PDF uncertainties at small  $x$ , and this is interpreted as a theoretical uncertainty. As such it is probably most appropriate to add this to the experimental PDF uncertainty linearly. However, as with other theoretical uncertainties it is impossible to gauge a confidence level. In principle a smooth GM-VFNS choice which also gives the best fit should provide the central value. I would

then consider the full variation of GM-VFNS definitions in this article as somewhat conservative, and very likely to be more than a one sigma uncertainty. At NNLO there is much greater stability, showing the success of the GM-VFNS approach, and the theoretical uncertainty is much smaller than the experimental PDF uncertainty. One of these GM-VFNS choices is extremely smooth near the transition point, a particular improvement at NLO, and reduces to *exactly* the correct asymptotic limits. It also gives a better fit quality, particularly at NLO, and less variation in the preferred  $m_c$  value between NLO and NNLO. This so-called “optimal” scheme seems to be a preferred option for global fits in future than the current default scheme used in the TR’ definition, which was chosen originally simply for simplicity and continuity, and I recommend this new alternative for future global PDF fits.

## Acknowledgements

I would like to thank A. D. Martin, W. J. Stirling and G. Watt for numerous discussions on PDFs, and S. Forte, P. Nadolsky and F. Olness for discussions on the topic of variable flavour number schemes. This work is supported partly by the London Centre for Terauniverse Studies (LCTS), using funding from the European Research Council via the Advanced Investigator Grant 267352.

## References

- [1] F. D. Aaron *et al.* [H1 and ZEUS Collaboration], JHEP **1001** (2010) 109 [arXiv:0911.0884 [hep-ex]].
- [2] E. Laenen, S. Riemersma, J. Smith and W. L. van Neerven, Nucl. Phys. B **392**, 162 (1993).
- [3] M. Buza, *et al.*, Eur. Phys. J. C **1** (1998) 301 [arXiv:hep-ph/9612398].
- [4] I. Bierenbaum, J. Blumlein and S. Klein, Nucl. Phys. B **820** (2009) 417 [arXiv:0904.3563 [hep-ph]].
- [5] J. Ablinger, J. Blumlein, S. Klein, C. Schneider and F. Wissbrock, Nucl. Phys. B **844** (2011) 26 [arXiv:1008.3347 [hep-ph]].
- [6] I. Bierenbaum, J. Blumlein and S. Klein, PoS D **IS2010** (2010) 148 [arXiv:1008.0792 [hep-ph]].
- [7] M. Gluck, E. Reya and M. Stratmann, Nucl. Phys. B **422** (1994) 37.
- [8] M. A. G. Aivazis, J. C. Collins, F. I. Olness and W. K. Tung, Phys. Rev. D **50** (1994) 3102 [arXiv:hep-ph/9312319].
- [9] R. S. Thorne and R. G. Roberts, Phys. Rev. D **57** (1998) 6871 [arXiv:hep-ph/9709442].
- [10] M. Buza and W. L. van Neerven, Nucl. Phys. B **500** (1997) 301 [arXiv:hep-ph/9702242].



- [11] R. S. Thorne and R. G. Roberts, Eur. Phys. J. C **19** (2001) 339 [arXiv:hep-ph/0010344].
- [12] A. D. Martin, W. J. Stirling, R. S. Thorne and G. Watt, Eur. Phys. J. C **70** (2010) 51 [arXiv:1007.2624 [hep-ph]].
- [13] S. Dittmaier *et al.* [ LHC Higgs Cross Section Working Group Collaboration ], [arXiv:1101.0593 [hep-ph]].
- [14] M. Cacciari, M. Greco and P. Nason, JHEP **9805** (1998) 007 [hep-ph/9803400].
- [15] M. Kramer, F. I. Olness and D. E. Soper, Phys. Rev. D **62** (2000) 096007 [hep-ph/0003035].
- [16] R. S. Thorne and W. K. Tung, arXiv:0809.0714 [hep-ph].
- [17] A. Chuvakin, J. Smith and W. L. van Neerven, Phys. Rev. D **61** (2000) 096004 [arXiv:hep-ph/9910250].
- [18] W. K. Tung, S. Kretzer and C. Schmidt, J. Phys. G **28** (2002) 983 [arXiv:hep-ph/0110247].
- [19] R. S. Thorne, Phys. Rev. D **73** (2006) 054019 [arXiv:hep-ph/0601245].
- [20] S. Forte, E. Laenen, P. Nason and J. Rojo, Nucl. Phys. B **834** (2010) 116 [arXiv:1001.2312].
- [21] M. Guzzi, P. M. Nadolsky, H. L. Lai and C. P. Yuan, arXiv:1108.5112 [hep-ph].
- [22] P. M. Nadolsky and W. K. Tung, Phys. Rev. D **79** (2009) 113014 [arXiv:0903.2667 [hep-ph]].
- [23] S. Alekhin, J. Blumlein, S. Klein and S. Moch, Phys. Rev. D **81** (2010) 014032 [arXiv:0908.2766 [hep-ph]].
- [24] S. Alekhin and S. Moch, Phys. Lett. B **699** (2011) 345 [arXiv:1011.5790 [hep-ph]].
- [25] S. Alekhin, J. Blumlein and S. Moch, arXiv:1202.2281 [hep-ph].
- [26] R. D. Ball *et al.*, Nucl. Phys. B **849** (2011) 296 [arXiv:1101.1300 [hep-ph]].
- [27] R. D. Ball *et al.* [The NNPDF Collaboration], arXiv:1107.2652 [hep-ph].
- [28] R. S. Thorne, PoS **DIS2010** (2010) 053 [arXiv:1006.5925 [hep-ph]].
- [29] A. D. Martin, W. J. Stirling, R. S. Thorne and G. Watt, Eur. Phys. J. C **63** (2009) 189 [arXiv:0901.0002 [hep-ph]].
- [30] A. D. Martin, W. J. Stirling, R. S. Thorne and G. Watt, Eur. Phys. J. C **64** (2009) 653 [arXiv:0905.3531 [hep-ph]].
- [31] J. R. Andersen *et al.* [SM and NLO Multileg Working Group Collaboration], arXiv:1003.1241 [hep-ph].

- [32] W. K. Tung, H. L. Lai, A. Belyaev, J. Pumplin, D. Stump and C. P. Yuan, JHEP **0702** (2007) 053 [arXiv:hep-ph/0611254].
- [33] E. Laenen and S. O. Moch, Phys. Rev. D **59** (1999) 034027 [arXiv:hep-ph/9809550].
- [34] S. Catani, M. Ciafaloni and F. Hautmann, Nucl. Phys. B **366** (1991) 135.
- [35] N. A. L. Presti, H. Kawamura, S. Moch and A. Vogt, PoS **DIS2010** (2010) 163 [arXiv:1008.0951 [hep-ph]].
- [36] H. Kawamura, N. A. Lo Presti, S. Moch and A. Vogt, Nucl. Phys. B **864** (2012) 399 [arXiv:1205.5727 [hep-ph]].
- [37] A. M. Cooper-Sarkar, A. Glazov, K. Lipka, R. Placakyte, V. Radescu, “QCD Analysis of Combined H1 and ZEUS F2c Data ”, H1prelim-10-143 ZEUS-prel-10-019.